



Open Archive Toulouse Archive Ouverte (OATAO)

OATAO is an open access repository that collects the work of Toulouse researchers and makes it freely available over the web where possible.

This is an author-deposited version published in: <http://oatao.univ-toulouse.fr/>
Eprints ID: 6786

To link to this article: DOI: 10.1007/s10443-011-9241-8
URL: <http://dx.doi.org/10.1007/s10443-011-9241-8>

To cite this version: Njionhou, Alvine and Berthet, Florent and Castanié, Bruno and Bouvet, Christophe *Relationships between LRI process parameters and impact and post-impact behaviour of stitched and unstitched NCF laminates*. (2012) *Applied Composite Materials*, vol. 19 (n° 6). pp. 885-899. ISSN 0929-189X

Any correspondence concerning this service should be sent to the repository administrator: staff-oatao@inp-toulouse.fr

Relationships Between LRI Process Parameters and Impact and Post-Impact Behaviour of Stitched and Unstitched NCF Laminates

Alvine Njionhou • Florentin Berthet • Bruno Castanié •
Christophe Bouvet

Abstract The general context of the development of out-of-autoclave processes in the aeronautics industry raises the question of the possible links between these new processes and impact behaviour. In this study, a Taguchi table was used in a design of experiment approach to establish possible links. The study focused on the liquid resin infusion process applied to laminates made with stitched or unstitched quadri-axial carbon Non-Crimp Fabric (NCF). On the basis of previous studies and an analysis of the literature, five process parameters were selected (stitching, curing temperature, preform position, number of highly porous media, vacuum level). The impact energy was set at 35 J in order to obtain enough residual dent depth. The parameters analysed during and after impact were: maximum displacement of the impactor, energy absorbed, permanent indentation depth, and delaminated surface. Then, compression after impact tests were performed and the corresponding average stress was measured. The interactions found by statistical analysis show a very high sensitivity to stitching, which was, of course, expected. A very significant influence of curing temperature and a significant influence of preform position were also found on the

A. Njionhou • F. Berthet
Ecole des Mines d'Albi (EMAC), Campus Jarlard, 81013 Albi cedex 09, France

A. Njionhou
e-mail: anjionho@mines-albi.fr

F. Berthet
e-mail: florentin.berthet@mines-albi.fr

B. Castanié (✉)
INSA, 135 Avenue de Rangueil, 31077 Toulouse Cedex, France
e-mail:bruno.castanie@insa-toulouse.fr

C. Bouvet
ISAE, 10 Avenue Edouard Belin, 31055 Toulouse Cedex, France
e-mail: christophe.bouvet@isae.fr

A. Njionhou • F. Berthet • B. Castanié • C. Bouvet
Université de Toulouse, INSA, UPS, Mines d'Albi, ISAE, ICA (Institut Clément Ader), Toulouse, France

permanent indentation depth and a physical explanation is provided. Globally, it was demonstrated that the resin infusion process itself did not influence the impact behaviour.

Keywords Liquid Resin Infusion · Non-Crimp Fabric · Impact · Compression after impact

Nomenclature

C_o	Stitching process parameter
N_{HPM}	Number of High Porous Media (HPM) process parameter
C_p	Plate side process parameter
T_c	Curing temperature process parameter
V_L	Vacuum level process parameter
E_a	Energy absorbed during impact
E_e	Elastic energy
S_d	Delaminated surface
δ_{max}	Maximum displacement of the impactor
α_p	Residual dent depth

1 Introduction

The development of aerospace composite structures today has to include a requirement for economic competitiveness. Thus, special attention is paid to out-of autoclave processes. While many technologies are in the running [1], liquid resin infusion (LRI) was selected for this study as it seems to be one of the most promising technologies because of its ease of use. The LRI process makes it possible to obtain composites of good quality [2, 3] for the aeronautics field. The classic epoxy resin type RTM 6 is used here for infusion. In the aeronautics context, it is necessary to size the composite structures according to the damage tolerance philosophy [4]. The sensitivity of epoxy layered structures to low velocity/low energy impact is high and can cause considerable loss of mechanical properties [5–8]. The objective of this research was therefore to determine whether the LRI process had an influence on the impact responses of these structures or not.

Given the great difficulty of establishing a direct relationship between process parameters and mechanical responses of manufactured parts, the design of experiment method was chosen. The nature of the preform is of paramount importance for both the manufacturing process and mechanical responses to impact. In a global cost-saving research context, it seems that there are advantages to the use of quadri-axial NCF layers, which enable productivity gains. Moreover, this new material remains poorly studied [9–13] especially under impact [14–17].

The techniques of through-thickness reinforcements (TTR) are also promising because, a priori, they improve mechanical properties, in particular on impact [18, 19]. Their main mode of action is to increase in the interlaminar strength of laminates. However, these techniques are intrusive. They generate spaces between the fibres, which have an influence on the resin flow during injection. Their influence on the mechanical properties studied in this research is not known. Two main reinforcement techniques are used: stitching [16–18] and Z-Pinning [19–21]. In our opinion, the second technique is particularly difficult to implement. It is also expensive and seems less promising than the second, which was used for this study. So the presence or absence of stitching will be considered as an input parameter for the design of experiment methodology. The choice of other parameters will be explained in the following section. Then the specimen manufacturing method will be

shown. Specific tests associated with the impact issue will be explained. Results of the experimental plan and associated statistical analysis will then be given. Each significant effect identified will be discussed in a later part.

2 Choice of Process Parameters, Experimental Plan and Manufacturing of Specimens

A search for theoretical and experimental approaches in the literature was made to identify the key process parameters that have the greatest impact on the performance and quality of infused composite structures [22–25]. These parameters were classified and grouped into three sets.

“Nature of preform” refers to the number of carbon NCF layers and the presence of stitching. It is reported to have an influence on the quality and mechanical properties of composites, and on the structure thickness, during the manufacturing process through flow of resin and during resin curing. Unlike in previous experiment plans [26, 27], for the sake of simplicity, composite plates were manufactured and tested with only one symmetric stacking sequence of 4 quadri-axial carbon NCF layers. These fabrics were provided by SAERTEX [28] and had a surface density of 1088 g/m². The final laminate thickness was approximately 4 mm. Thus, the only parameter of the “*nature of preform*” set was the presence or absence of stitching (C_o). It was set to its low value of -1 (no) or its high value of 1 (yes) in the experimental plan. A similar system of “low value/high value” was applied for the other parameters.

The second set was the process configuration. It included the vacuum level (V_L) achieved in the vacuum cavity during the resin injection process, the number of High Porous Media (HPM) layers used (N_{HPM}), which is a characteristic parameter for the flow of resin during structure manufacturing by LRI, and the side of the composite plate on the mould during the infusion process (C_p), “vacuum side” or “injection side”. The vacuum level represents the absolute pressure in the vacuum cavity. It cannot be imposed and varies according to the assembly. The “vacuum level” (V_L) has been found to be a crucial parameter for the quality of composite materials [29–31] in the vacuum infusion process. The values of vacuum level shown in the experimental plan (Table 1) are those obtained during the manufacture of composites according to each configuration. Furthermore, research has proved that the use of

Table 1 Experiment plan

Process conditions		Process parameters				
N°	Exp.	Stitching	Curing Temp. (°C)	Number of HPM	Plate side	Vacuum Level (mbar)
1	CAI 1 V	No	180	1	Vacuum	1.3
2	CAI II	No	180	1	Injection	1.3
3	CAI 2 V	No	160	2	Vacuum	1.4
4	CAI 2I	No	160	2	Injection	1.4
5	CAI 3 V	Yes	180	2	Vacuum	1.6
6	CAI 3I	Yes	180	2	Injection	1.6
7	CAI 4 V	Yes	160	1	Vacuum	1.4
8	CAI 4I	Yes	160	1	Injection	1.4
9	CAI 5 V	Yes	170	2	Vacuum	1.3
10	CAI 5I	Yes	170	2	Injection	1.3

HPM (in this study Aerovac Ref VI5, 100 g/m², polyamide with a fibre ratio of 13%) or the number of its layers in the configuration could influence the properties of the composite in its own right, or by interaction with the number of layers of fibre reinforcement [22, 31]. It was also shown in [27] that the number of HPM has an influence on the thickness of the laminate. An increase of 0.08 mm was observed with 2 HPM. The recent identification of this parameter as an impact factor and its integration into analysis should enable better control of its effects on the variation of properties. To manufacture infused composite structures, 1 or 2 HPM with a permeability of $4 \times 10^{-10} \text{ m}^2$ were used. The position of the structure relative to the resin inlet is also a factor of variability of composite properties as the velocity field of resin flow in the mould depends on the location of the structural preform and the number and positions of the resin inlets and outlets. Variation of the field might cause the formation of different type, shape or size of voids in the composites [30–33] and would have an influence on the integrity of a composite structure. This could have effects on the fibre volume fraction and void content of the composite part as well as on its mechanical properties. Thus, the plate side of the composite “ C_p ”, “vacuum side or injection side” is used in this study to quantify the influence of the position of specimens during manufacturing on the mechanical properties of the structure (see Fig. 1).

The temperatures used during the manufacturing process could also generate variability of the morphological and mechanical properties of the final composites, by their influence on the viscosity of the resin and its flow velocity through the preform and during the resin curing. The process temperatures form the 3rd set. From a theoretical point of view, this set concerns mould temperature, injection temperature and curing temperature. These parameters were taken into account in a previous experimental plan [27]. However, it was found that only the curing temperature of the part had very significant effects on the morphological properties of the infused laminates. To diminish the size of the experimental plan, only this parameter was studied here. The curing temperature (T_c) of the part was 160°C for the lower bound and 180°C for the upper bound. The other temperatures were fixed at 80°C for the resin injection and 100°C for the mould initial temperature.

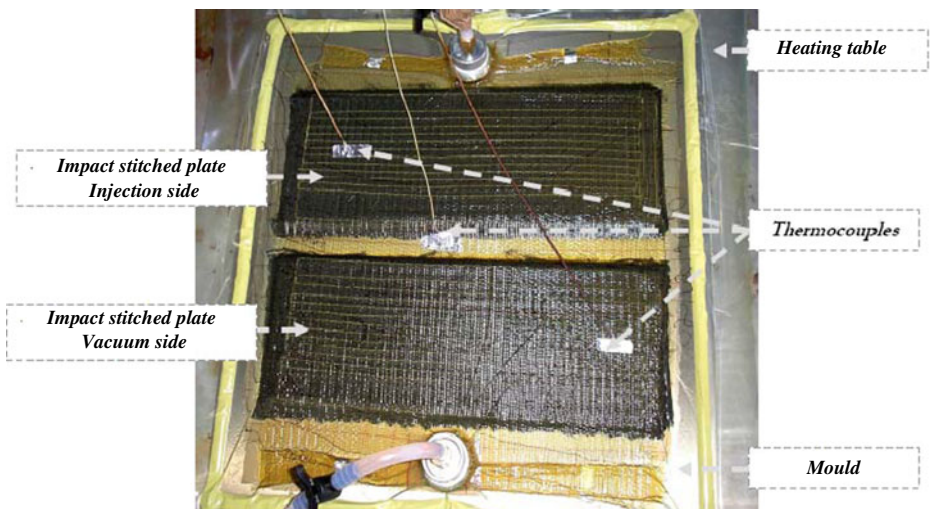


Fig. 1 LRI manufacturing of two stitched plates

The experimental plan was a table of Taguchi type $L_8 (2^7)$ which has 5 columns of process parameters and 8 lines of manufacturing experiments (Tab 1). Two additional lines were added to this table to enable a verification of the results in the statistical analysis. After cutting ($400 \times 150 \text{ mm}^2$) and stacking of the NCF layers, some preforms were stitched. The stitching was done lengthwise in parallel straight lines. A modified lock stitch method with Kevlar thread was used. The length between two successive points and the spacing between two lines was 8 mm. The preforms were placed as shown in Fig. 1 before infusion.

The vacuum device was activated until a vacuum level of less than 2 mbar was reached. For each experiment, liquid resin was systematically heated in a resin pot and degassed under vacuum for 10 min. This operation took place before the resin was passed into an injection tube and infused into the preform at 80°C . The infusion process continued until the resin reached the exit port. The same vacuum level was maintained until the end of manufacturing. Then the RTM6 curing cycle was applied followed by cooling at ambient temperature (around 20°C). In order to keep the curing temperature effects in the laminate, no post-curing was carried out. Subsequently, the plates were cut to the size of Airbus standard AITM 1-0010 ($150 \times 100 \text{ mm}^2$) relating to impact and compression after impact tests. For the stitched plates, a minimum distance of 6 mm between the stitch line the edge of the plate was observed. A total of 60 specimens were made so as to have 6 plates per configuration.

3 Tests and Measurements

Impact tests were carried out using a drop weight device [7]. The mass was guided in a vertical tube. The impacted plate was maintained by a clamping window. The impact energy was set according to the BVID (Barely Visible Impact Damage) criterion. This notion corresponds to a dent detectable in service by airlines and is the cornerstone of the philosophy of damage tolerance. It is recognized that a dent of 0.2 to 0.3 mm is detectable at 2 m distance, while a dent of 0.1 mm is only detectable by detailed inspection. In this study, several successive impact tests were conducted on supernumerary plates to obtain a residual dent of 0.3 mm, thus above the BVID. By this method, the impact energy was set at 35 joules, which is finally of the same order of magnitude as in [2]. This energy corresponds to an impact velocity of about 4 m/s for the impactor mass.

During this test, the instantaneous speed and contact force were measured. From these data, the instantaneous displacement was computed and the load/displacement curves drafted. The *maximum displacement* (δ_{max}) of the impactor during impact and the energy absorbed by the structure (E_a) were computed from the experimental force/displacement curves (Fig. 2). This energy corresponds to the surface described by the hysteresis curve. The area under the return curve is the elastic energy (E_e) of the structure. Theoretically, $E_a + E_e = 35 \text{ J}$.

The residual dent depth (α_p) was measured 24 h after the test because of a relaxation phenomenon. Measurements were taken on a surface area of $110 \times 60 \text{ mm}^2$ of the specimen with a grid of $5 \times 5 \text{ mm}$. The maximum value obtained was the value of the permanent indentation. The projected delaminated surface area (S_d) was measured by C-scan. Figure 3 shows two delamination patterns for stitched and unstitched plates. After these measurements, the widths of impacted plates were machined again (grinding) to obtain good parallelism. This operation was indispensable to obtain a good compression field in the specimen. The tests were performed on a 45-ton SCHENCK machine. The plates were

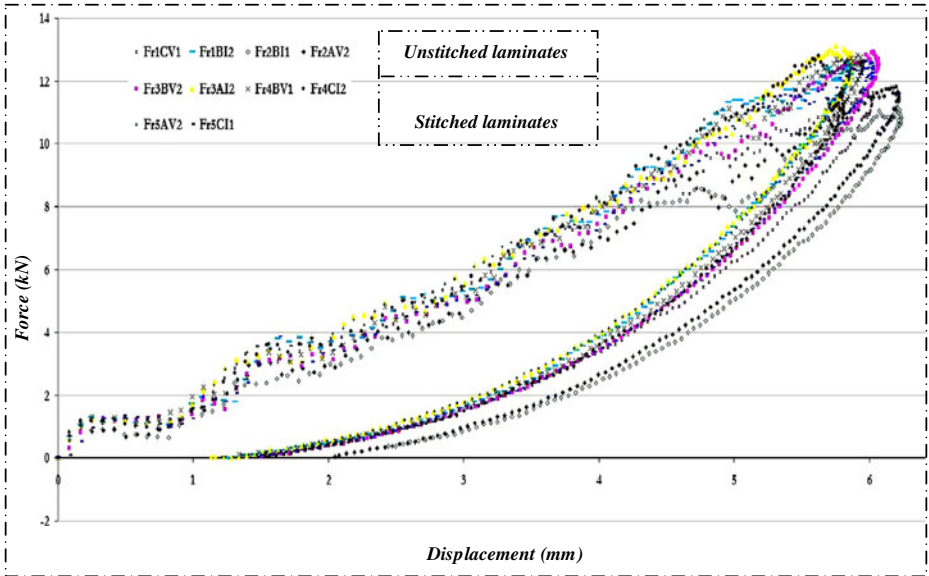


Fig. 2 Force versus displacement curves during impact

inserted in a specific device developed to meet Airbus standard AITM 1-0010 [7]. Knives were used on each side of the specimen to prevent the onset of global buckling of the specimens before compression failure. Even after resurfacing, mounting the specimen was a very delicate stage and was very important to ensure the quality of the test. Thus, all specimens were equipped with six strain gauges mounted face to face. This allowed the test to be tracked and misalignment, manifested by a bending captured by the gauges, to be prevented (Fig. 4). Initial loading was applied up to 25% of the final load and the asymmetry

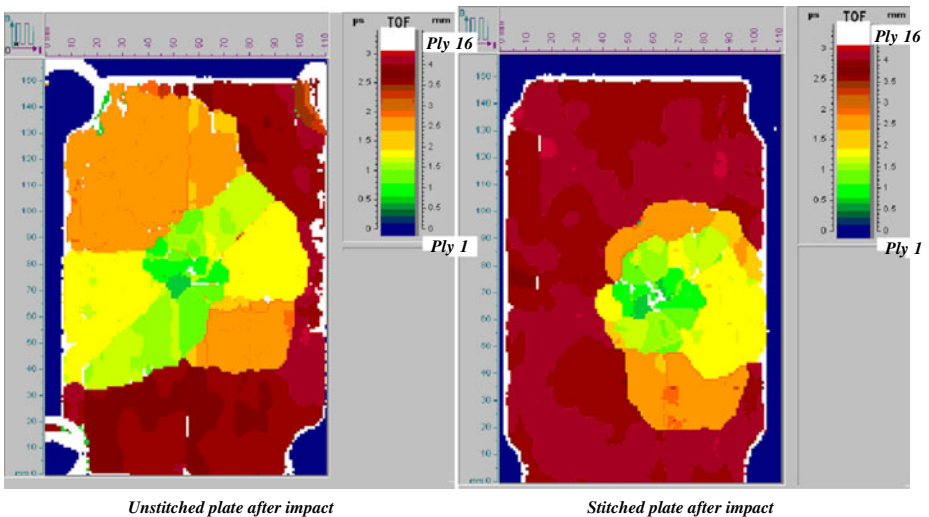


Fig. 3 Delamination patterns after impact

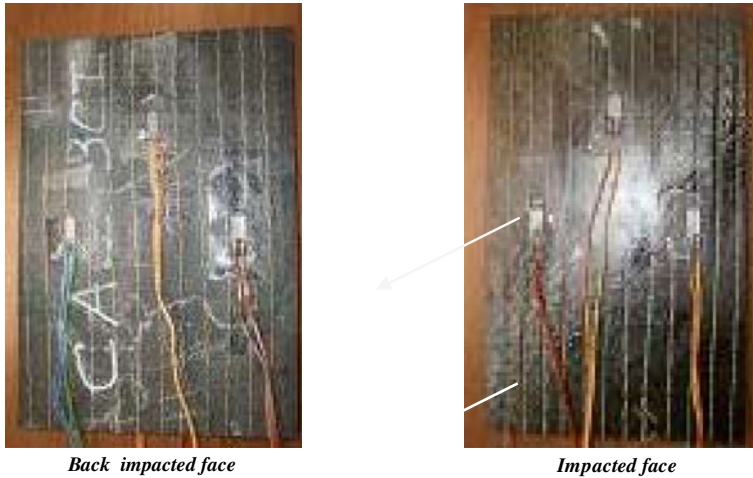


Fig. 4 Location of the strain gauges for compression-after-impact test

of the gauges was evaluated. This asymmetry should not exceed 10%. Thus, it was not uncommon to proceed to three assembly/disassembly/realignment steps prior to rupture. The test was conducted at a speed of 0.01 mm/s. The average maximum stress at failure in CAI (σ_{CAI}) was calculated simply by dividing the maximum force by the cross section of the specimen.

4 Experimental Results and Analysis

4.1 Experimental Results

The properties measured after the 60 impacts and the compression after impact tests are summarized in Tables 2 and 3. Each value is the average of 6 tests and the standard deviation is given. In this table, the elastic energy is also given, which verifies the validity of the tests because the sum $E_a + E_e$ is equal to the 35 joules of impact energy. A quick analysis of raw data showed that the impact characteristics were best for stitched laminates, as expected. Only a statistical analysis was able to highlight less trivial links.

4.2 Statistical Analysis

The linear expression of the general model of the experimental plan is Eq. 1. It was obtained by multilinear regression. Equations 2–7 represent the models found for each property studied: maximum displacement of the impactor (δ_{max}), residual dent depth (α_p), absorbed energy (E_a), elastic energy (E_e), delaminated surface area (S_d) and compression strength after impact (RCAI). Each of these equations depends on parameters that are very significant (VS) or significant (S) for the result. The influential parameters can take the value -1 or 1 . For the lower value of influential parameters (-1), we obtained minimum responses, while encoding to 1 (high value of parameter)

Table 2 Average of impact properties

Process Conditions			Impact properties (Average)									
N°	Exp.		Defl. δ_{max} (mm)	Dev (δ_{max})	Dent α_p (mm)	Dev (α_p)	Absorbed Energy E_a (J)	Dev (E_a)	Elastic Energy E_c (J)	Dev (E_c)	Delaminated area S_d (mm ²)	Dev (S_c)
Unstiched	1	CAI 1 V	5.98	0.30	0.45	0.10	20.25	0.99	15.71	0.77	6916.00	639.56
	2	CAI 1I	5.85	0.44	0.46	0.04	19.29	0.87	15.99	1.05	6057.33	1273.70
	3	CAI 2 V	6.34	0.30	0.56	0.08	20.37	1.25	15.76	1.08	6727.67	834.30
	4	CAI 2I	6.28	0.30	0.50	0.07	19.60	1.33	15.61	1.29	7686.33	578.37
Stiched	5	CAI 3 V	6.36	0.67	0.42	0.09	18.75	0.67	17.20	0.64	5801.33	1308.07
	6	CAI 3I	5.92	0.21	0.38	0.07	18.33	1.41	17.00	1.22	6259.83	1536.98
	7	CAI 4 V	5.95	0.03	0.50	0.03	18.77	1.34	17.72	1.02	4942.00	690.82
	8	CAI 4I	5.77	0.06	0.40	0.06	19.13	0.87	15.93	0.65	5603.83	488.94
	9	CAI 5 V	5.89	0.08	0.43	0.06	19.02	1.04	17.28	0.84	4837.83	190.46
	10	CAI 5I	6.07	0.16	0.42	0.05	19.69	1.75	16.50	1.09	5199.83	922.06
Average (Lines 1 to 8)			6.06		0.45		19.29		16.36		6154.72	

gave property values that were considered maximum. Thus, an unstitched infused laminate absorbs an energy of 19.86 J and has a maximum compressive strength after

Table 3 Average of compression-after-impact strength

Process Conditions		Compression after impact	
N°	Exp.	RCAI (MPa)	Deviation (RCAI)
1	CAI 1V	148.11	6.23
2	CAI 1I	154.19	15.49
3	CAI 2V	146.42	12.24
4	CAI 2I	138.75	3.33
5	CAI 3V	189.58	5.73
6	CAI 3I	182.44	22.48
7	CAI 4V	182.42	6.87
8	CAI 4I	188.36	7.46
9	CAI 5V	183.12	10.59
10	CAI 5I	187.31	22.64
Average (lines 1 to 8)		166.89	

impact of 147.21 MPa versus 18.74 J and 185.67 MPa respectively for a stitched infused laminate (Eqs. 4 and 7). Results of the analysis are shown below:

$$Y = C + a_{C_0} \cdot C_0 + a_{T_c} \cdot T_c + a_{N_{HPM}} \cdot N_{HPM} + a_{C_p} \cdot C_p + a_{V_L} \cdot V_L \quad (1)$$

$$\delta_{max} = 6.06 + 0.16 N_{HPM} - 0.10 C_p \quad (2)$$

$$\alpha_p = 0.46 - 0.03 C_0 - 0.03 T_c - 0.03 C_p \quad (3)$$

$$E_a = 19.30 - 0.56 C_0 \quad (4)$$

$$E_e = 16.35 + 0.59 C_0 \quad (5)$$

$$S_d = 6135.47 - 533.42 C_0 + 433.63 N_{HPM} \quad (6)$$

$$RCAI = 166.44 + 19.23 C_0 \quad (7)$$

Table 4 shows that, as expected, the effect of the stitching is very significant for the mechanical properties and morphology related to impact. These results are consistent with the literature and will be detailed in the following paragraphs. Other process parameters appeared more unexpectedly, in particular permanent indentation depth. This issue will be analysed separately.

4.3 Stitching Influence

The results of statistical analysis given in the previous subsection are summarized in Fig. 5. Stitching causes a decrease of: indentation depth of 0.07 mm (-14%), absorbed energy of 1.13 J (-5.6%), and delaminated surface area of about 10.67 cm² (-16%). In contrast, stitched laminates have a higher compressive strength after impact of 38.45 MPa (+26%) compared to unstitched. These results are a “structure” effect provided by out-of-plane reinforcement due to stitching, which is quite expected. These results found by statistical

Table 4 Synthesis of influence of process parameters on impact properties and CAI

Analysis Parameters	Impact and post-impact properties					
	δ_{max}	α_p	E_a	E_e	S_d	RCAI
Stitching (C_0): « no » to « yes »		VS (-)	VS (-)	VS (+)	VS (-)	VS (+)
Number of HPM (N_{HPM}): From 1 to 2	VS (+)				VS (+)	
Plate Site (C_p): From vacuum to injection side	S (-)	S (-)				
Vacuum level (N_v): Low to High						
Curing Temperature (T_c): From 160°C to 180°C	f	VS (-)				

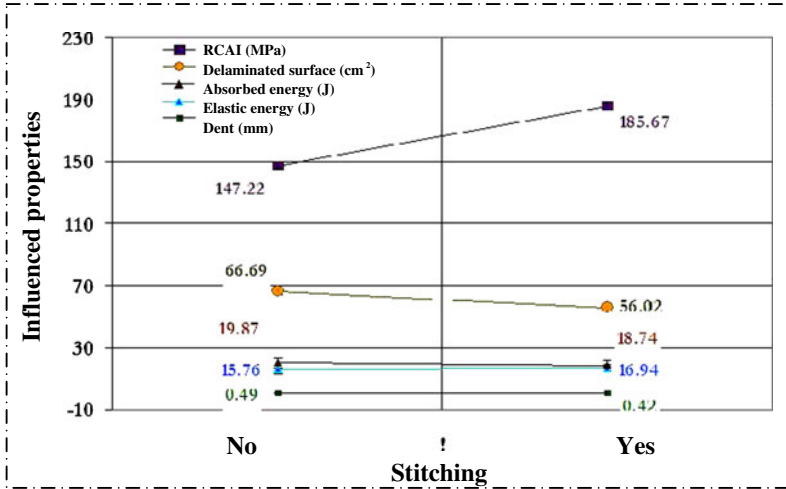


Fig. 5 Statistical results related to the influence of stitching on the impact and after-impact properties

analysis are logical because a structure that absorbs less energy will be less suitable for the propagation of damage. In addition, it is interesting to link the delaminated area to RCAI (Fig. 6). A notable drop-off in residual strength can be observed when the delaminated area increases. This result is also consistent with the literature.

Analysis by C-Scan of delaminated surfaces illustrated the differences between stitched and unstitched plates. In most cases, damage created by impact on these laminates extends to

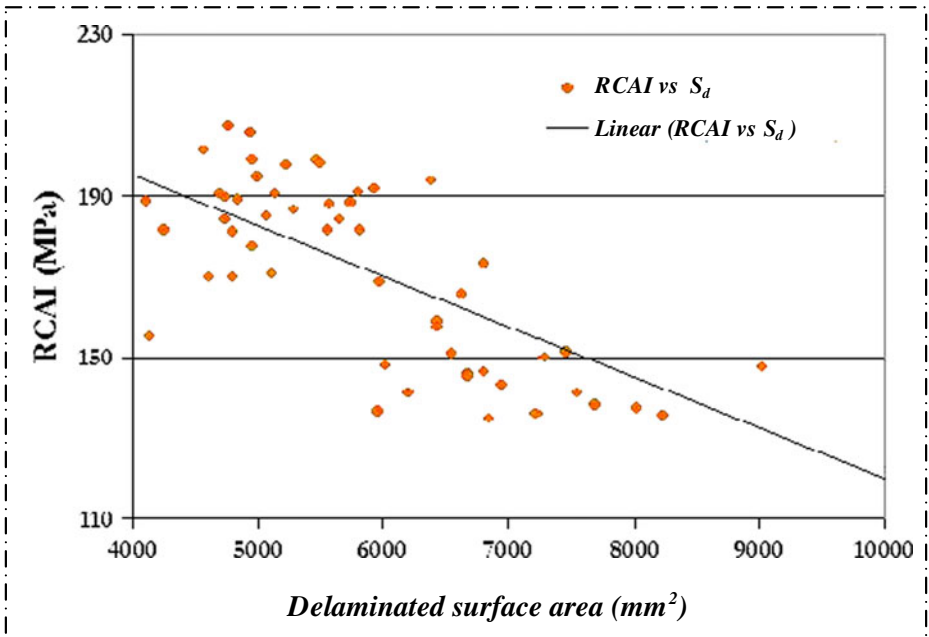


Fig. 6 Experimental results of RCAI according to the delaminated area

the edge. This phenomenon is even more pronounced for unstitched plates (Fig. 3). There is also a loss of symmetry of the map of delaminations when they “touch” the edge of the plate. Significant increases in delamination area occur at interfaces between quadri-axial NCF. It has been shown by microscopic observations [10] that these interfaces are resin-rich areas which should promote the growth of local delaminations. Thus, it is logical that the presence of stitching points strengthens this interface, limiting the overall extent of the delaminated area. The presence of resin-rich areas is also found in the autoclave process; it is a phenomenon related to the intrinsic rigidity of quadriaxial NCF [9–11].

4.4 Influence of Number of HPM

The number of high porous media used in the process had a very significant influence on the maximum displacement of the impactor during the impact test (δ_{max} , Eq 2) and on the delaminated surface area of the structure (S_d , Eq. 6). These two properties increased by 0.34 mm (+5.8%) and 8.67 cm² (+15.2%) respectively (Fig. 7). This result therefore indicates that the use of two porous media to manufacture infused laminate with 4 NCF encourages the propagation of damage within the structure. In a previous experimental plan [27], the lowest fibre content and thus the highest rates of matrix were obtained for the same process configuration with 4 NCF and 2 HPM. Also, it was shown that, for this configuration, due to a low infusion speed, macro-porosities were created. This type of defect can obviously facilitate the creation of intralaminar matrix cracks. Moreover, in impact, inter-laminar matrix cracks are precursors to delamination [5]. We can therefore assume that this process configuration can promote the creation of such cracks and so increase the phenomenon of delamination, thus ultimately increasing the delaminated area. The link between the number of HPM and the fact that the maximum deflection is higher is probably due to the increase in delaminated area, which generates a lower bending stiffness on impact and therefore a greater maximum deflection.

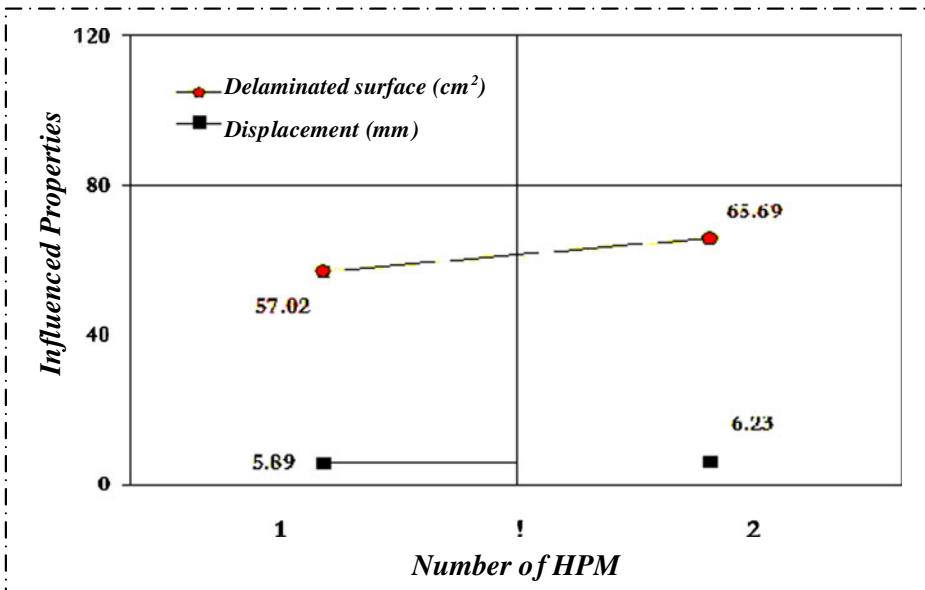


Fig. 7 Effect of number of HPM on the impact properties of infused laminates

4.5 Effect of Process Parameter on Residual Dent

Statistical analysis showed that the plate side and curing temperature process parameters had significant or very significant effects on the permanent indentation depth. Equation 3 shows that dents were 13% deeper on the vacuum side and decreased by 10.4% when the curing temperature rose from 160°C to 180°C. The link may seem difficult to establish, but we propose the following explanation in relation to a previous result of the laboratory. It has been shown that, in the case of a highly oriented laminate, a debris blocking phenomenon occurred in the matrix cracks and prevented springback after impact [34]. This phenomenon enables the creation of the residual dent. As for HPM influence, it was shown in a related part of this study [26, 27] that the vacuum side and the temperature generated a significant presence of macro-porosities (see Fig. 8). Moreover, these macro-porosities were largely located in resin-rich areas (Fig. 9). Also, these defects were more pronounced with 4 layers of NCF. If we follow the assumption that the residual indentation is related to a phenomenon of debris blocking (Fig. 10) in the voids left by the matrix cracks, there is a strong presumption that the presence of these initial cavities promotes this phenomenon and therefore generates deeper indentations. The fact that the experimental plan method has identified a link between these parameters seems to confirm the hypothesis of debris blocking.

5 Conclusions

A study to establish links between infusion process parameters of NCF laminates and their impact and after-impact properties was performed. An experimental plan was designed using an L₈Taguchi table (2⁷). Infused laminates were impacted using a drop weight device at low energy (35 J) and low speed (4 m/s) to obtain a residual indentation depth of around 0.3 mm

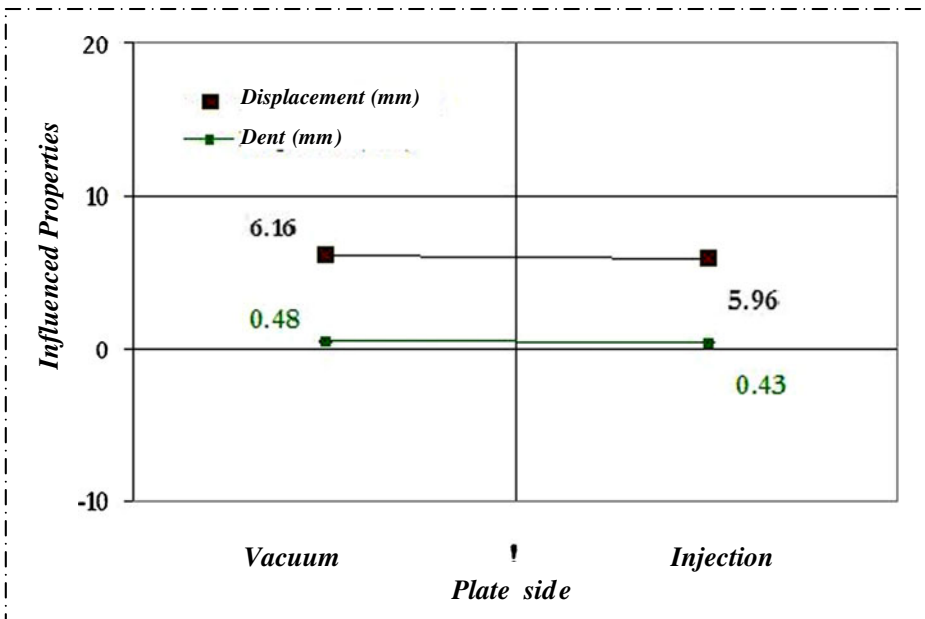
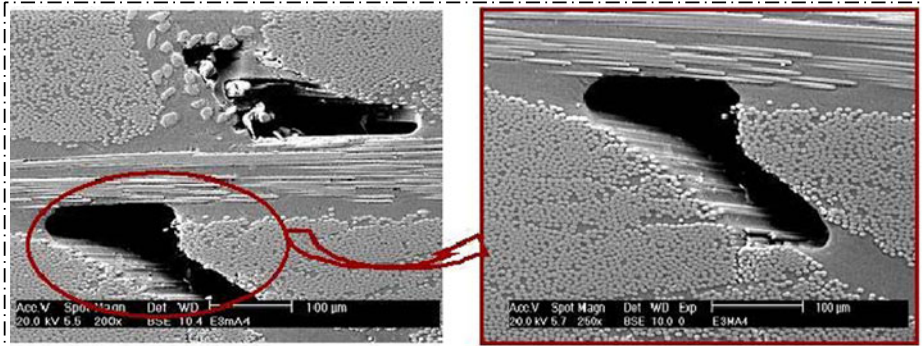
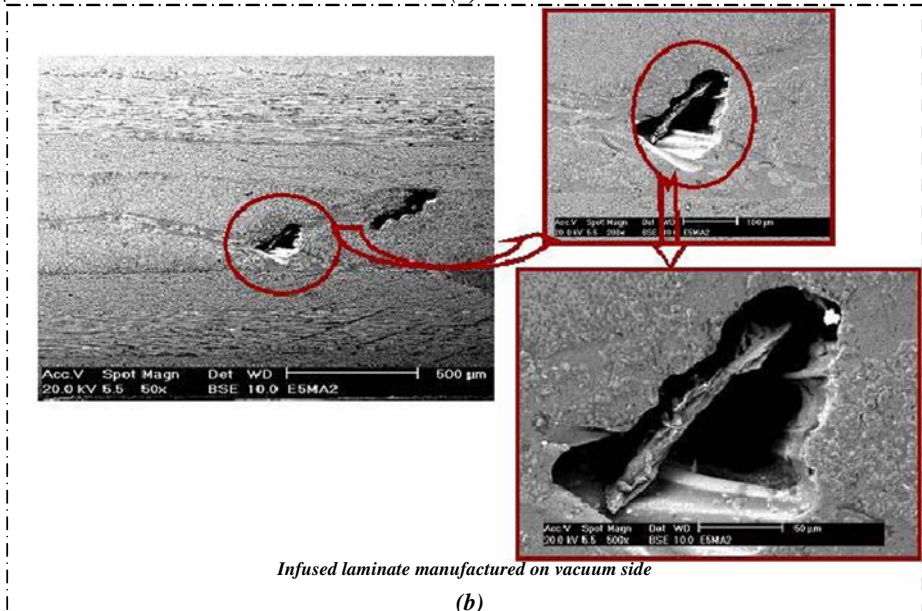


Fig. 8 Effect of plate side on impact properties of infused laminates



Infused laminate manufactured with high curing temperature

(a)



Infused laminate manufactured on vacuum side

(b)

Fig. 9 Examples of macro-porosity obtained inside infused laminate manufactured: with high curing temperature (a) and on vacuum side (b)

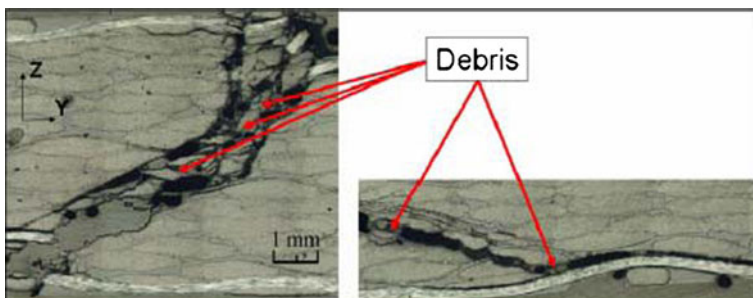


Fig. 10 Example of debris blocking (reproduced from [27])

(above the BVID). Properties in impact and compression after impact (CAI) were subsequently analysed statistically. Morphological analyses were also completed and enabled links to be established with damage patterns. Consistently with the literature, stitching was the main process parameter affecting the impact parameters, with only one exception (the maximum displacement of the impactor). Stitching reduces overall energy absorption of the laminate. This phenomenon results in the limitation of the extension of damage by decreasing the delaminated area. The consequence is the increase the strength after impact of infused laminates. It is also shown that the compression strength decreases when the delaminated area increases. Non-destructive analyses (ultrasonic C-scan and binocular microscopy) were performed on the impacted laminates to support these comments. Significant damage propagation was observed. Moreover, a loss of symmetry of the mapping of delaminations was found and seemed to be due to interaction with the edges. The experimental plan method established a strong link between some process parameters and the permanent indentation depth. The level of these parameters corresponds to the creation of local macro-porosities, thus facilitating the creation of interlaminar cracks during the impact. According to the experience of our laboratory, permanent indentation is due to a blocking of debris in these matrix cracks. Overall, apart from this residual dent, the study showed that the method of manufacture by resin infusion itself had no significant effect on the impact behaviour of laminates made by this out-of-autoclave process.

References

1. Beckwith, S.W.: Resin infusion liquid molding vacuum infusion processing numerous other names. An Alphabet Soup Expanding Technologies. *SAMPE Journal* **42**(1) (2006).
2. Takeda, F., Nishiyama, S., Hayashi, K., Komori, Y., Suga, Y., Asahara N.: Research in the Application of the VARTM Technique to the Fabrication of Primary Aircraft Composite Structures. Mitsubishi Heavy Industries. *Technical Review* **42**(5) (2005)
3. Casari, P., Stervinou, B., Davies, P., Choqueux, D.: Process-mechanical properties relationship for an aircraft wing spar: comparison of prepreg, LRI and RFI techniques. FPCM-9, 9th International Conference on Flow Processes in Composite Materials Montréal (Québec), Canada 8–10 July 2008
4. Fualdes, C., Morteau, E.: Composite@Airbus – Damage Tolerance Methodology. FAA Workshop for Composite Damage Tolerance and Maintenance, Chicago IL, July 19–21, 2006
5. Bouvet, C., Castanić, B., Bizeul, M., Barrau, J.-J.: Low velocity impact modelling in laminate composite panels with discrete interface elements. *Int J Sol Struct* **46**, 2809–2821 (2009)
6. Abrate, S.: *Impact on Composites Structures*. Cambridge University Press, (1998)
7. Petit, S., Bouvet, C., Bergerot, A., Barrau, J.J.: Impact and compression after impact of a composite laminate with a cork thermal shield. *Comp. Sci. Tech.* **67**, 3286–3299 (2007)
8. De Freitas, M., Reis, L.: Failure mechanisms on composite specimens subjected to compression after impact. *Comp. Struct.* **42**, 365–373 (1998)
9. Lundstrom, T.S.: The permeability of non-crimp stitched fabrics. *Comp. Part A* **31**, 1345–1353 (2000)
10. Mattsson, D., Joffe, R., Varna, J.: Methodology for characterization of internal structure parameters governing performance in NCF composites. *Comp. Part B* **38**, 44–57 (2007)
11. Drapier, S., Wisnom, M.R.: Finite-element investigation of the compressive strength of non-crimp-fabric-based composites. *Comp. Sci. Tech.* **59**, 1287–1297 (1999)
12. Edgren, F., Asp, L.E., Joffe, R.: Failure of NCF subjected to combined compression and shear loading. *Comp. Sci. Tech* **66**, 2865–2877 (2006)
13. Koissin, V., Kustermans, J., Lomov, S.V., Verpoest, I., Van Den Broucke, B., Witzel, V.: Structurally stitched NCF Preforms: Quasi-Static response. *Comp. Sci. Tech* **69**, 2701–2710 (2009)
14. Asp, L.E., Juntikka, R.: High velocity impact on NCF reinforced composite. *Comp. Sci. Tech* **69**, 1478–1482 (2009)
15. Vallons, K., Behaeghe, A., Lomov, S.V., Verpoest, I.: Impact and Post-Impact properties of carbon fibre non-crimp fabric and a twill weave composite. *Comp. Part A* **41**, 1019–1026 (2010)
16. Heb, H., Himmel, N.: Structurally stitched NCF CFRP laminates. Part 1: Experimental characterization of in-plane and out-of-plane properties. *Comp. Sci. Tech.* **71**, 549–568 (2011)

17. Heb, H., Himmel, N.: Structurally stitched NCF CFRP laminates. Part 2: Finite element unit cell based prediction of in-plane strength. *Comp. Sci. Tech.* **71**, 569–585 (2011)
18. Mouritz, A.P., Leong, K.H., Herszberg, I.: A review of the effect of stitching on the in-plane mechanical properties of fibre-reinforced polymer composites. *Comp. Part A* **28A**, 979–991 (1997)
19. Mouritz, A.P.: Review of Z-pinned composite laminates. *Comp. Part A* **38**, 2383–2397 (2007)
20. Toral Vasquez, J., Castanié, B., Barrau, J.J., Swiergel, N.: Multi-level analysis of low-cost z-pinned composite junctions, part 1: single z-pin behavior. *Comp. Part A* **42**, 2070–2081 (2011)
21. Toral Vasquez, J., Castanié, B., Barrau, J.J., Swiergel, N.: Multi-level analysis of low-cost z-pinned composite junctions, part 2 Joint behavior. *Comp. Part A* **42**, 2082–2092 (2011)
22. Teemer, L., Okoli, O. I., Liang, Z.: The effect of processing parameters on the mechanical properties of components manufactured using the Resin Infusion between Double Flexible Tooling Process. *SAMPE'06 Long Beach April*, **51** (2006)
23. Lawrence, J.M., Neacsu, V., Advani, S.G.: Modeling the impact of capillary pressure and air entrapment on fiber tow saturation during resin infusion in LCM. *Comp. Part A* **40**, 1053–1064 (2009)
24. Trochu, F., Ruiz, E., Achim, V., Soukane, S.: Advanced numerical simulation of liquid composite molding for process analysis and optimization. *Comp. Part A* **37**, 890–902 (2006)
25. Ruiz, E., Trochu, F.: Comprehensive thermal optimization of liquid composite molding to reduce cycle time and processing stresses. *Polym. Comp.* **26**, 209–230 (2005)
26. Njionhou, A., Berthet, F., Castanié, B.: Optimisation de la résistance au cisaillement interlaminaire (RCIL) des matériaux composites fabriqués par LRI en fonction des paramètres de fabrication. *Mat. Tech* **98**, 151–163 (2010)
27. Njionhou, A., Berthet, F., Castanié, B.: Relationships between process parameters and mechanical properties of composite made by L.R.I. 10th International Conference on Flow Processes in Composite Materials (FPCM10) Monte Verità, Ascona, CH – July 11–15, 2010
28. SAERTEX Datasheet.: Description of style quadriaixial-carbon-fabric PB/PE. SAERTEX GmbH&Co (2005)
29. Yenilmez, B., Senan, M., Sozer, E.M.: Variation of part thickness and compaction pressure in vacuum infusion process. *Comp. Sci. Tech.* **69**, 1710–1719 (2009)
30. Govignon, Q., Bickerton, S., Morris, J.: Full field monitoring of the resin flow and laminate properties during the resin infusion process. *Comp. Part A* **39**, 1412–1426 (2008)
31. Dong, C.: A modified rule of mixture for the vacuum-assisted resin transfer moulding process simulation. *Comp. Sci. Tech.* **68**, 2125–2133 (2008)
32. Lee, C.-L., Wei, K.-H.: Effect of material and process variables on the performance of resin-transfer-molded epoxy fabric composites. *J. Appl. Polym. Sci.* **77**, 2149–2155 (2000)
33. Pearce, N.R.L.: An investigation into the effects of fabric architecture on the processing and properties of fibre reinforced composites produced by resin transfer moulding. *Comp. Part A* **29**, 19–27 (1998)
34. Abdallah, E., Bouvet, C., Rivallant, S., Barrau, J.J.: Experimental analysis of damage creation and permanent indentation on highly oriented plates. *Comp. Sci. Tech.* **69**, 1238–1245 (2009)